

Incorporating Power Electronic Converters Reliability into Modern Power System Reliability Analysis

Saeed Peyghami, *Member, IEEE*, Frede Blaabjerg, *Fellow, IEEE*, Peter Palensky, *Senior Member, IEEE*

Abstract— This paper aims to incorporate the reliability model of power electronic converters into power system reliability analysis. The converter reliability has widely been explored in device- and converter-levels according to physics of failure analysis. However, optimal decision-makings for design, planning, operation and maintenance of power electronic converters require system-level reliability modeling of power electronic-based power systems. Therefore, this paper proposes a procedure to evaluate the reliability of power electronic based power systems from the device-level up to the system-level. Furthermore, the impact of converter failure rates including random chance and wear-out failures on power system performance in different applications such as wind turbine and electronic transmission lines is illustrated. Moreover, due to a high calculation burden raised by the physics of failure analysis for large scale power electronic systems, this paper explores the required accuracy for reliability modeling of converters in different applications. Numerical case studies are provided employing modified versions of the Roy Billinton Test System (RBTS). The analysis shows the converter failures may affect the overall system performance depending on its application. Therefore, an accurate converter reliability model is, in some cases, required for reliability assessment and management in modern power systems.

Index Terms—reliability, wind farm reliability, wear-out failure, converter reliability, adequacy, HVDC reliability.

I. INTRODUCTION

Electric power system modernization is essential for reliable and secure power delivery with low to zero carbon footprint. It requires deploying new technologies and infrastructure as well as deregulating the electricity sector. Some established technologies have a considerable role in power systems modernization including renewable energy resources, storages, electronic transmission and distribution systems, and e-mobility. Notably, power electronics plays an underpinning role in energy conversion process of aforementioned technologies [1]. Particularly, moving toward one hundred percent renewable energies has intensified the importance of power electronics in future power systems. However, power converters are one of the frequent source of failures in many applications [2]–[4], hence introducing high downtime and maintenance costs [2]–[10]. Moreover, according to field data and industrial experiences, the power converters are exposed to aging and wear-out failures depending on the operating conditions [3]–[5], [11], [12].

A power converter is made up of various sub-systems including power modules, capacitors, gate drivers, control units, and cooling system. Electrolytic capacitors and power modules are the two most fragile components which are also prone to wear-out failure. The reliability of these components depends on different factors such as device mechanical strength, applied electrical load, climate conditions, control and switching schemes. These factors cause degradation of component materials during long-term operation of the converter, finally triggering potential failure mechanisms. Physics of failure-based Stress-Strength Analysis (SSA) for different failure mechanisms can be used for component reliability prediction and enhancement from wear-out standpoint.

The SSA requires electro-thermal modeling in three hierarchical levels including device-level, converter-level and system-level [13]. The system-level modeling identifies the loading of the converter according to its application in the power system. For instance, the loading of parallel-connected converters depends on power sharing strategies. Moreover, the converter-level studies include the electrical domain modeling and simulations in order to find out the stress of each components under applied control and switching strategies. Finally, the device-level analysis requires electro-thermal modeling of devices for obtaining key thermal variables, such as hot-spot temperature, which are enabling failure mechanisms under a given mission profile. As a result, the SSA analysis comprise very fast dynamics in the range of switching frequency at the device-level to the slow dynamics in the range of hourly load changes at the system-level. Therefore, the wear-out failure prediction over an annual mission profile is a time-consuming process. In the system-level analysis it will introduce very high calculation burden specially in large-scale power systems.

So far, the SSA has been employed in device-level for lifetime modeling and extension in capacitors and semiconductor devices [14]–[19]. In the converter-level, the SSA is used for converter lifetime extension by active thermal management approaches such as appropriate modulation strategies [20]–[22], adaptive switching frequency [23], and active/reactive power control [24]–[26]. The converter topologies and photovoltaic array characteristics are other factors affecting the converter lifetime [22], [27], [28]. Furthermore, the capacitors lifetime expansion is explored in [28], [29] by interleaving the converters. Moreover, the system-level reliability enhancement in multi converter systems is performed by appropriately modifying the converters loading and shifting the device damages form high-stressed converter to the low-stressed one [13], [30].

The aforementioned reliability analyses in [13]–[30] are limited to the converter lifetime prediction and enhancement even at the system-level studies. However, optimal decision-making in design, planning, operation and maintenance of the converters in the power systems requires to analyze their impacts on power system reliability. This requires bridging the power electronic reliability concepts and the power system reliability assessment approaches.

The power system reliability is defined as a measure of its ability to cope with customer demands [31]. Technically, this ability is measured by adequacy indices such as Loss OF Load Expectation (LOLE) and Expected Energy Not Supplied (EENS) [31]. Besides the conventional power systems reliability analysis [31], the reliability of power electronic-based power systems such as Wind Farms (WFs) and High Voltage Direct Current (HVDC) transmission systems have been widely studied, e.g., in [31]–[42]. In the state-of-the-art research [31], [32], [41], [42], [33]–[40], the failure rate of converters in power system analysis is obtained from the historical data of similar cases. Moreover, the wear-out failure

of converters has not been taken into account in the power system reliability assessment. In practice, the wear-out of converter components may happen earlier than the expected lifetime [11]. Therefore, not only the failure rate of converter during operation will be increased, but also its end-of-life will be limited. Hence, the converter components aging will affect the overall system reliability and risk, consequently inducing higher downtime and maintenance costs specially in the large-scale power electronic-based power systems.

In order to avoid these issues, appropriate strategies must be adopted for optimal decision-making in planning, operation and maintenance of modern power electronic-based systems. This requires system-level reliability analysis by incorporating the converter reliability modeling in power system reliability assessment. This procedure is very time-consuming, and in practice, for large-scale power systems is almost impossible. This is due to the fact that the electro-thermal modeling based on SSA requires time-domain analysis with the time frame of interest from microsecond associated to the converter switching frequency up to the hourly load variations. Therefore, system-level reliability modeling in power electronic-based systems needs simplified electro-thermal modeling techniques in different time frames.

According to the aforementioned issues posed by proliferation of converters in power systems, this paper aims to address the following challenges:

- 1) Since any decision-making regarding converters operation, planning and maintenance must be performed at the system-level, hence, the system-level reliability modeling in power electronic-based systems is of high importance. This paper aims at bridging the converter reliability models and power system reliability concepts for evaluating the reliability of power electronic-based power systems.
- 2) Due to the increasing use of converters in power systems, their failure rates associated with the random chance and wear-out failures may affect the overall performance of power systems. This paper will illustrate the impact of converter failures and aging on the power system reliability.
- 3) Due to the complexity of the reliability modeling in converters based on SSA, the simplified approaches should be introduced for system-level analysis. This paper presents the required accuracy of converter reliability modeling for power system analysis in different applications.
- 4) The converter failure rate will be increased due to the aging of components. Thereby, they must be replaced according to a suitable maintenance strategy. The impact of run-to-fail and age replacement policies on the power system reliability is presented in this paper.

In order to achieve the above-mentioned goals, Section II represents the reliability modeling in power electronic converters. The reliability evaluation in power systems and incorporation of converter reliability in power system analysis are presented in Section III. Numerical analyses are provided in Section IV. Finally, the outcomes are discussed and summarized in Sections V and VI.

II. CONVERTER RELIABILITY MODELING

The failure characteristics of a converter, like other systems, comprises three periods including infant mortality, useful lifetime and wear-out phase as shown in Fig. 1. Usually, the infant mortality failures are related to the debugging and

manufacturing processes. Hence, the converter will experience the random chance and wear-out failures within operation. The random chance failure rate is usually predicted based on the historical reliability data and operational experiences. Moreover, the wear-out failure rate is modeled by SSA over the aging prone components.

Following field data, the power modules (i.e., semiconductor devices) and capacitors are the most fragile converter components. The lifetime model of the electrolytic capacitors is obtained by [43]:

$$L_o = L_n \cdot 2^{\frac{T_n - T_o}{n_1}} \left(\frac{V_o}{V_n} \right)^{-n_2}, \quad (1)$$

where, L_n is the nominal lifetime under nominal voltage V_n and upper category temperature T_n , and L_o is the capacitor lifetime under operating voltage V_o and temperature T_o . The exponents of n_1 and n_2 are obtain by lifetime testing [43]. Furthermore, the number of cycles to failure, N_f in semiconductor devices is calculated by using [44]:

$$N_f = A \cdot \Delta T_j^\alpha \cdot \exp\left(\frac{\beta}{T_j}\right) \cdot \left(\frac{t_{on}}{1.5}\right)^{-0.3}, \quad (2)$$

where, ΔT and T are the junction temperature swing and its average value, and t_{on} denotes the rise time of temperature cycle. The constants of A , α , and β are curve fitting constants obtained from aging tests [44].

In order to obtain the lifetime of the devices, the annual mission profile should be translated into thermal variables in (1) and (2), i.e., temperature, and voltage, through electro-thermal analysis. This procedure is shown in Fig. 2(a). Therefore, the detailed electrical and thermal model of converter components must be employed which requires time-domain analysis. After translating the mission profile to the thermal variables, the thermo-mechanical damage of the devices must be calculated to predict the converter lifetime. Accumulated Damage of the Capacitors (AD_C) under a given mission profile is obtained as:

$$AD_C = \sum_k \frac{t_k}{L_{o-k}}, \quad (3)$$

where, t_k is the period that the capacitor operates under (V_o , T_o), and L_{o-k} is the corresponding lifetime obtained by (1).

Moreover, in order to obtain the Accumulated Damage of Semiconductor devices (AD_S), the junction temperature profile is classified into different classes, where the class h is defined as a set of variables (T_h , ΔT_h , t_{on-h} , $n_{cycle-h}$). The AD_S is then obtained as:

$$AD_S = \sum_h \frac{n_{cycle-h}}{N_{f-h}} \quad (4)$$

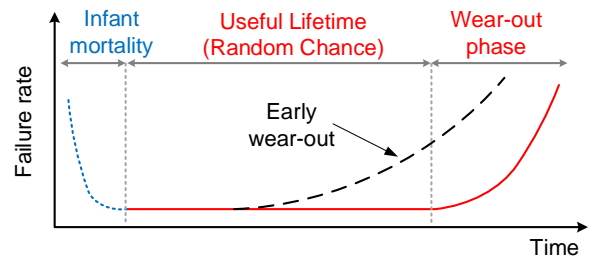


Fig. 1. Typical failure shape of an item known as bathtub curve.

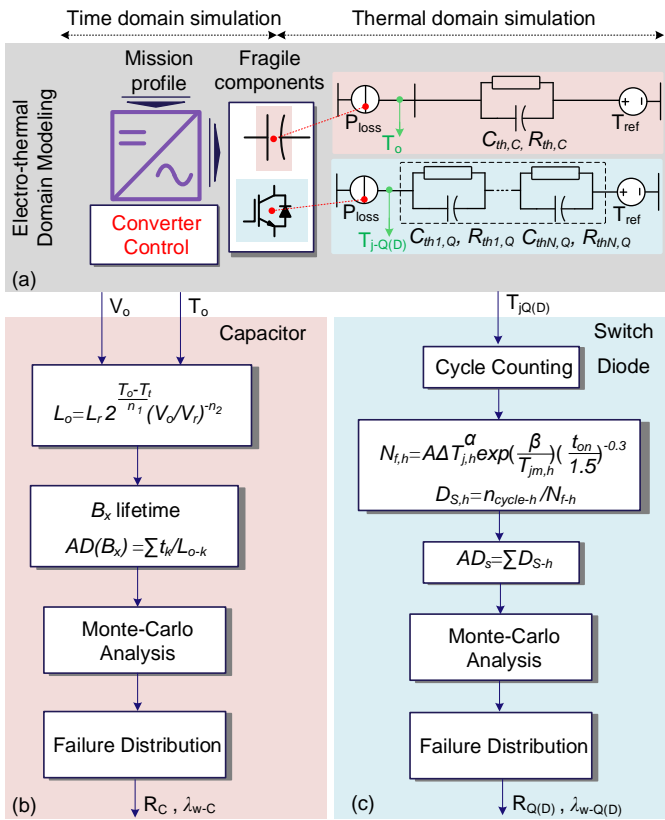


Fig. 2. Wear-out failure rate prediction in power converters, (a) electro-thermal mapping, (b) wear-out failure rate of capacitors and (c) wear-out failure rate of semiconductor devices.

where, $n_{cycle-h}$ is the number of cycles in class h and N_{f-h} is the corresponding number of cycles. The device lifetime is equal to the reciprocal of the AD in (3) and (4). The obtained AD values for each devices are associated with the specific values of lifetime models in (1) and (2) as well as specific thermal models of devices. In practice, the lifetime models and device thermal characteristics have uncertainties with a certain range of variations. Therefore, the distribution of AD in terms of model and manufacturing uncertainties must be identified. The AD distribution function can be obtained by Monte-Carlo simulations as shown in Fig. 2 (b & c). The reciprocal of the AD distribution function is known as the device unreliability function, $F(t)$. Once, the unreliability function is obtained, the wear-out failure rate of components can be calculated as:

$$\lambda_{w-X} = \frac{1}{1-F(t)} \frac{d}{dt} F(t), \quad (5)$$

where, d/dt is the differential operator and λ_{w-X} denotes as the wear-out failure of device X . Usually, the wear-out failure rate is modeled by a Weibull distribution function with a hazard function of $h(t)$ as:

$$h(t) = \lambda_{w-X} = \beta \alpha^{-\beta} t^{\beta-1}, \quad (6)$$

where, α and β are the scale and shape factors of Weibull distribution. Finally, the device X failure rate λ_X is obtained by using:

$$\lambda_X = \lambda_{w-X} + \lambda_{c-X}, \quad (7)$$

where, λ_{c-X} denotes as the constant failure rate within useful lifetime, which can be predicted based on historical failure data and operational experiences.

III. POWER SYSTEM RELIABILITY

Power system reliability, so-called adequacy is a measure of its ability to meet the electric power and energy requirements

of the customers within acceptable technical limits considering the component outages [45]. The main measure employed in power system reliability assessment is the availability of its components. Availability is defined as the probability that an item is in operating state at any instant t given that it started to operate at instant zero. This section will present the general concept of components availability with time-constant and time-varying failure rates. Moreover, the reliability of power systems and its sub-systems will be presented.

A. Concept of Availability

Generally, the failure rate of components is considered constant (see Fig. 1) owing to the fact that they are regularly maintained and the wear-out rarely happens. It is worth to mention that a run-to-fail replacement strategy is employed for availability prediction in this paper. For exponentially distributed systems, the availability can be obtained by using the Markov Process (MP). Following MP, system states can be represented as being in operating state of “1” and being in down state “2” as shown in Fig. 3(a). The system availability, A according to the MP is the probability of being in state “1”, which is obtained as [46]:

$$A = 1 - FOR = \frac{\mu}{\lambda + \mu} \quad (8)$$

where λ, μ are the failure and repair rates within useful lifetime respectively. Forced Outage Rate (FOR) is defined as the unavailability following (8).

For the systems with non-exponential failures, the MP cannot be utilized. In this case, the failure rate can be decoupled into constant and time-varying terms. The cause of random chance failures in converter components such as capacitors and semiconductor devices are induced by abnormal operation and sudden over-stressing the components, while the wear-out failures are due to the long-term degradation of the component materials. Therefore, they have independent failure causes, and decoupling the failure rate into constant and time-varying terms is an appropriate assumption. As a result, a system with non-constant failure rate shown in Fig. 3(b) can be converted into two sub-systems with time-constant failure rate shown in Fig. 3(c) and time-varying term as shown in Fig. 3(d). According to Fig. 3(c & d), the system is available if and only if both sub-systems are available. Therefore, the total availability $A_t(t)$ can be obtained as:

$$A_t(t) = A_c \cdot A_w(t), \quad (9)$$

where, $A_c(t)$ is associated with the time-constant failure rate obtained by using (8). Moreover, the $A_w(t)$ is related to the time-varying failure rate with the Probability Distribution Function (CDF) of $F_{12}(t)$. In order to obtain the time-varying availability, the Semi-Markov Process (SMP) can be employed [47], [48]. According to SMP, The probability of being in state j if the process starts at state i , ζ_{ij} can be obtained by using (10) [47].

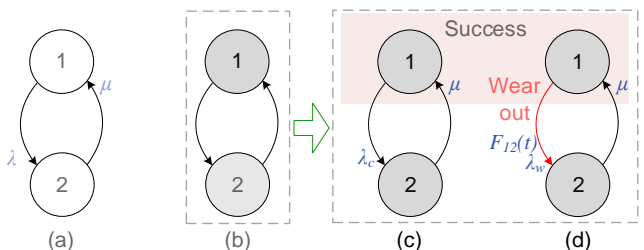


Fig. 3. State space modeling of single system; (a) Markov model with constant failure rates, (b) General model with non-constant failure rate, (c) Markov model of time-constant failure rate, and (d) semi-Markov model of time-varying failure rate.

$$\zeta_{ij}(t) = \delta_{ij}(1 - F_{ij}(t)) + \sum_{k=1}^2 \int_0^t \frac{d}{d\tau} F_{ik}(\tau) \cdot \zeta_{kj}(\tau - t) d\tau, \quad (10)$$

where δ_{ij} is:

$$\delta_{ij} = \begin{cases} 1 & i = j \\ 0 & i \neq j \end{cases}. \quad (11)$$

Following Fig. 3(d), $F_{12}(t)$ is the failure CDF and $F_{21}(t)$ is the repair CDF with constant repair rate of μ . According to (10), the availability of the sub-system with time-varying failure rate is equal to the probability of being in state “1” given that the process has been started to operate in state “1”, hence,

$$A_w(t) = \zeta_{11}(t). \quad (12)$$

B. Availability of power converters

The reliability of a converter can be modeled by its components reliability as shown in Fig. 4(a). Since switches and capacitors are prone to wear-out failures [2], [49], their availability is modeled individually by using (9). The converter is available if, and only if, all the components are available as shown in Fig. 4(b). Hence, the overall converter availability is obtained by using (13).

$$A_{con}(t) = A_{switch}(t) \cdot A_{cap}(t) \cdot A_o, \quad (13)$$

where, $A_x(t)$ is the instantaneous availability of $x = \text{switch, cap, Other components}$. $A_{switch}(t)$ and $A_{cap}(t)$ are predicted by SMP using (9) and $A_o(t)$ is predicted by MP using (8).

C. Availability of HVDC system

The HVDC system contains a sending end converter, a receiving end converter and a DC transmission line. The HVDC system reliability can be modeled as a series network of these components as shown in Fig. 5. Hence, the availability of the HVDC system, $A_{HVDC}(t)$ is calculated as:

$$A_{HVDC}(t) = A_{con}(t) \cdot A_{con}(t) \cdot A_{DC} \quad (14)$$

where $A_{con}(t)$ is the HVDC Converters (HC) availability obtained by using (13) and A_{DC} is the availability of DC line obtained by using (8).

D. Availability of wind turbine

A WT consists of different components such as blades, hub, generator, gear-box, converter, control [38]. Similar to the HVDC system, the availability of the WT, $A_{WT}(t)$ can be obtained as:

$$A_{WT}(t) = A_{con}(t) \cdot A_{OC} \quad (15)$$

where, $A_{con}(t)$ and A_{OC} denote the availability of WT Converter (WTC) and other components. Due to the uncertainty in wind power, its availability should also be included in the WT

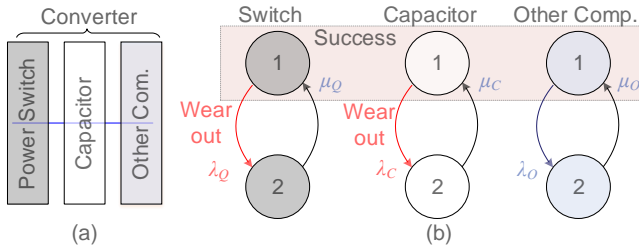


Fig. 4. Power converter reliability model; (a) reliability block diagram, (b) Markov model.

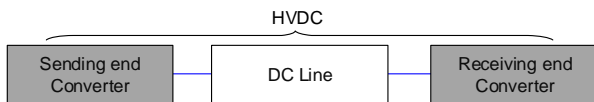


Fig. 5. HVDC system reliability model.

availability. One approach to model the wind power availability is to discretize the output power of the WT into some states. For instance, in a 2 MW WT, its output power can be divided into 0, 0.5, 1, 1.5, 2 MW as shown in Fig. 6. The probability of each state can be obtained by convolving the probability of wind power probability distribution with the WT characteristic curve [32], [37], [50]. Each state is available if the turbine is available. The availability of a 40 MW WF with twenty WTs can be obtained by combining the availability model of individual WT. Hence, the entire states will be 40, 39.5, 39, ..., 0 MW. Therefore, like the conventional generation system [31], the capacity outage probability can be calculated for the WF. The detail analysis has been discussed in [32], [37]. According to Fig. 9, the wind power is available in the grid side if, and only if, the HVDC transmission line, i.e., WF Converters (WFCs) and DC line is available. Therefore, the total probability of each state must be convolved with the availability of WF HVDC line.

E. Reliability of wind farm

The performance of a WF can be measured by its availability [51]–[53]. Two kinds of availability measures can be defined for WFs including time-based availability A_{time} [51] and production-based availability A_{prod} [52]. The annual time-based availability is obtained by:

$$A_{time} = 8760 \left(1 - \frac{\text{Unavailable time}}{\text{Available time} + \text{Unavailable time}} \right) [h/y] \quad (16)$$

Time-based unavailability is the complementary of the time-based availability. Moreover, the production-based availability is calculated as:

$$A_{prod} = 1 - \frac{\text{Lost production}}{\text{Actual energy production} + \text{Lost production}} \quad (17)$$

Furthermore, the reliability of a generation system, here a WF, can be measured by the Expected Energy Not Produced (EENP) due to the unavailability of WF components [54] as:

$$EENP = \sum_{i=1}^n \Psi_i \cdot (P_i^A - P_i^\mu) \cdot 8760 \quad (18)$$

where, Ψ_i is the WF capacity in state i , P_i^A is the probability of state i considering the WF components are fully available and P_i^μ is the probability of state i considering the unavailability of the WF components.

F. Reliability of power system

Power system reliability is measured by probabilistic indices such as Loss Of Load Expectation (LOLE) and Expected Energy Not Supplied (EENS) [31], [55]. These two indices are the most popular measures of power system adequacy, where the LOLE is the number of days or hours within a specific period of time in which the load cannot be supplied due to the generation shortage, and it is calculated as:

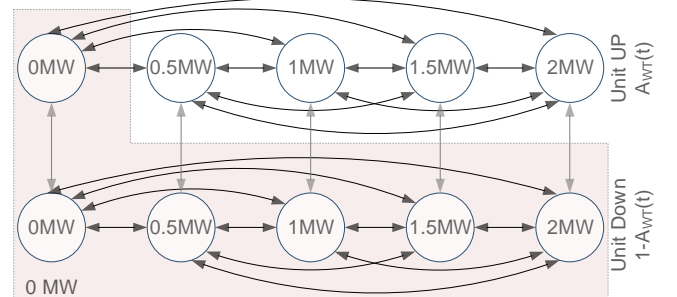


Fig. 6. A 2 MW WF reliability model – the highlighted states show zero generation.

$$LOLE = \sum_{i=1}^n P_i \cdot (C_i - L_i) \quad (19)$$

where C_i is the available capacity in interval i , L_i is the forecasted peak load, P_i is the portability of loss of load [31]. EENS is also defined as the curtailed energy due to the generation shortage and it is estimated by using (20) [56].

$$EENS = \sum_{i=1}^n P_i \cdot E_i \quad (20)$$

where E_i is the curtailed energy.

The flow of the reliability prediction in the power system is shown in Fig. 7. First, the wear-out failure rate of power converters of WT is predicted according on SSA under given mission profile for each WT. Afterwards, the WTC availability is estimated based on wear-out and random chance failure rates. Then, the availability of WT is estimated according to the availability of the WT components and wind power availability. The WF HVDC transmission line availability can also be predicted based on converters wear-out failure and historical data of random chance failures. Combining the availability of the WTs and the WF transmission line will result in WF reliability model and its availability. Furthermore, the HVDC transmission system availability can also be predicted based on the availability of transmission line reliability which is obtained by converters wear-out random chance failures. The availability of the conventional generators can also be modeled based on availability of individual units according to [31]. The overall generation system reliability model can be obtained by combining the reliability models of WFs, HVDC systems and conventional generators. Finally, the system reliability indices including LOLE and EENS are predicted by convolving the generation system reliability and the system load model.

IV. NUMERICAL ANALYSIS

In the modern power systems, the energy sources can be conventional generators, Wind Turbines (WTs), solar photovoltaic arrays, energy storage systems, and neighboring grids. In this paper, the reliability of two power system structures is evaluated. The first system is the modified RBTS with additional 40 MW and 4×40 MW WFs with 20% and 64%

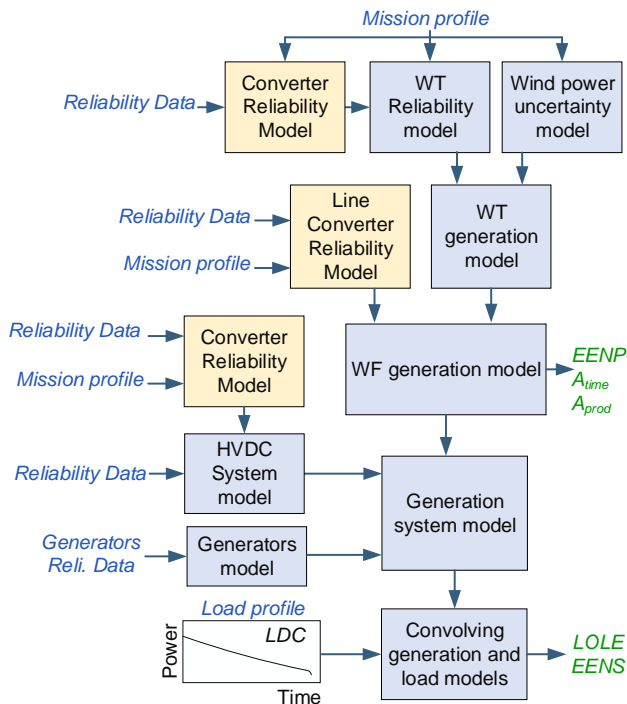


Fig. 7. Reliability evaluation in modern power systems.

wind penetration respectively. The structure of the modified RBTS is shown in Fig. 8. The RBTS information including reliability data and load model are provided in [57]. The structure of the 40 MW WF is shown in Fig. 9 including twenty 2 MW V80-2.0 WTs manufactured by Vestas Wind Systems with cut-in, rated, and cut-out speeds of 4, 15, and 25 m/s, respectively. The WF is connected to the grid through a DC transmission line. Wind speed data of two different location with resolution of one minute is utilized as shown in Fig. 10.

Moving toward one hundred percent renewable energies necessitates the power systems to interconnect into the neighboring grids. Therefore, the RBTS is further modified by interconnecting to the neighboring grids through three 100 MW HVDC lines as shown in Fig. 11. The modified RBTS is fully equipped with Power Electronics (PE), and it would be called modified PE-RBTS. In this case, it is assumed that the neighboring grids are always available and the local grid does not support the neighboring grids. In the following, the reliability of the two power systems is analyzed.

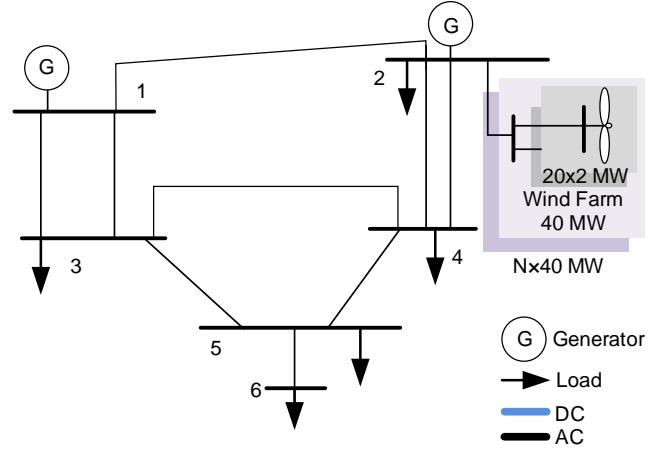


Fig. 8. Modified RBTS (The main version is provided in [57]), Wind Farm Converter (WFC).

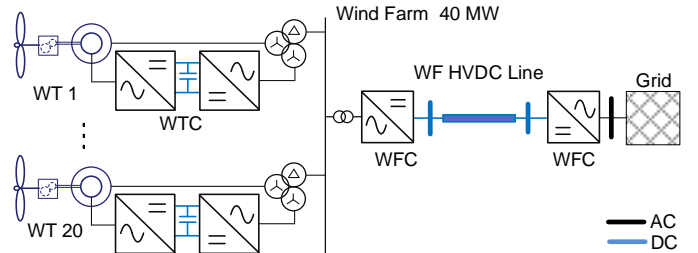


Fig. 9. A 40 MW DFIG based Wind Farm (WF) Structure with 20×2 MW Wind Turbines (WTs).

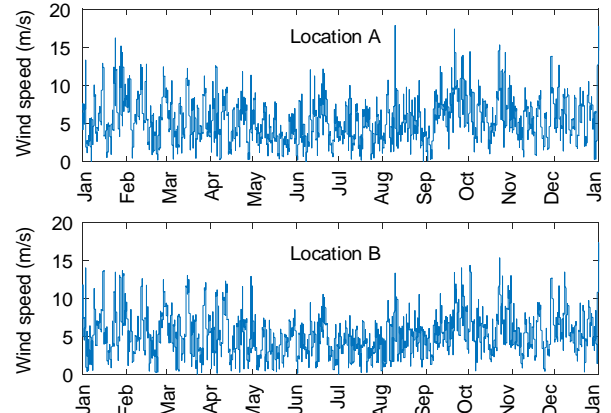


Fig. 10. Wind speed profile of two locations with one-minute resolution.

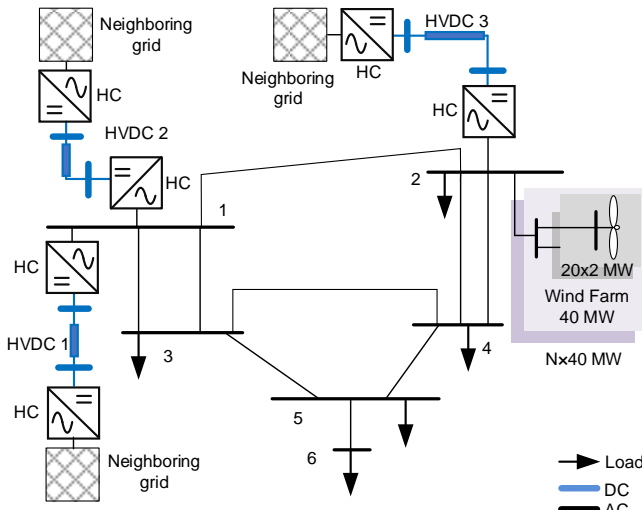


Fig. 11. Full Power Electronic based RBTS (PE-RBTS). HC: HVDC Converter.

A. Converter availability

The converter availability (or unavailability) depends on the random chance and wear-out failure rates. The random chance failure rate of converters is provided in Table APP-I in Appendix. Moreover, the wear-out failure rate is predicted based on SSA for the WT converter shown in Fig. 9 under the given mission profiles in Fig. 10. The converter structure and characteristics for a 2 MW DFIG-based WT is provided in [58] which includes a 0.4 MW partial-scale two-level converter. Since the thermal modeling and SSA of converters have been widely addressed in [22], [58]–[61], the detail modeling process is not represented here. Hence, the reliability prediction is carried out following the procedure described in Fig. 2, and the results are employed for system-level analysis. The wear-out failure rates are represented by a Weibull distribution as given in (6). Following SSA-based reliability prediction approach, the wear-out failure rate characteristics of the converter switches and capacitors are obtained as $(\alpha, \beta)_{\text{switch}} = (12, 3)$, $(\alpha, \beta)_{\text{cap}} = (10, 3)$ for mission profile of location A shown in Fig. 10 and $(\alpha, \beta)_{\text{switch}} = (8, 3)$, $(\alpha, \beta)_{\text{cap}} = (7, 2.6)$ for location B.

The converter components unavailability is predicted for both constant and time-varying failure rates using (9). Their unavailability due to the random chance failures and the total unavailability are shown in Fig. 12. The total converter unavailability due to the random chance failures is almost 0.007. It can be seen from Fig. 12 that the wear-out of converter components will increase its unavailability from 0.007 to 0.011. shape factors (α, β) . As a result, employing the random chance failure rate, and neglecting the impact of components aging will introduce error on the converter reliability. The unavailability of the HVDC converters of WF and transmission systems in the modified RBTS test systems can be predicted similar to this case, and the total unavailability can be used for system-level analysis.

B. Wind farm reliability

The WF reliability is evaluated employing the historical reliability data summarized in Table APP-I as a base case. These data are associated with the random chance failures. For the base case, the reliability indices are summarized in TABLE I, where the time-based unavailability is 168 h/y, the production-based availability is 97.0 % and the EENP is equal to 1,8550 MWh/y.

The impact of converter components wear-out on the performance of the 4×40 MW WF is illustrated in Fig. 13. The

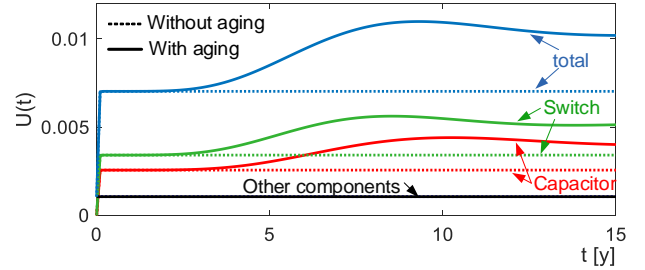


Fig. 12. Impact of component aging on the converter unavailability, $U(t)$; $(\alpha, \beta)_{\text{switch}} = (12, 3)$, $(\alpha, \beta)_{\text{cap}} = (10, 3)$.

TABLE I
Wind Farm (WF) reliability indices for the base case given in the Appendix.

WF	Time-U [h/y]	Prod-A [%]	EENP [MWh/y]
160 MW	168	97	18,550

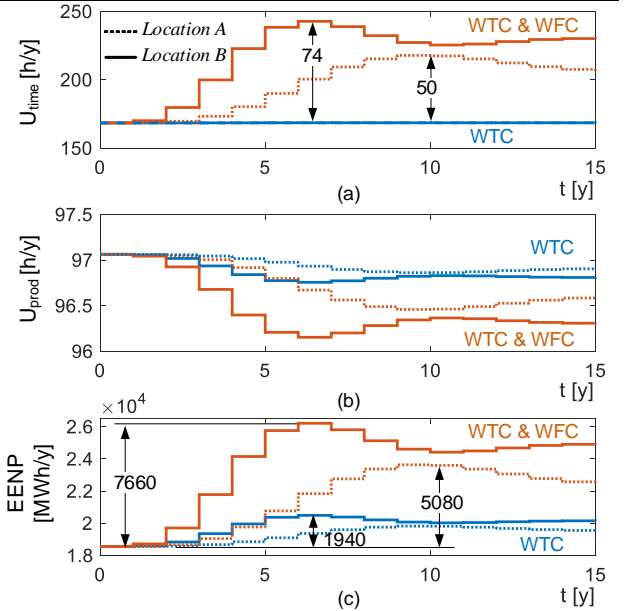


Fig. 13. Impact of WTC and WFC wear out on the reliability of 160 MW WF, (a) Time-based unavailability, (b) production-based unavailability, (c) EENP due to the wear-out of WFC or WTC.

wear-out characteristics of WTC under two mission profiles is $(\alpha, \beta)_{\text{switch}} = (12, 3)$, $(\alpha, \beta)_{\text{cap}} = (10, 3)$ for location A and $(\alpha, \beta)_{\text{switch}} = (8, 3)$, $(\alpha, \beta)_{\text{cap}} = (7, 2.6)$ for location B. Moreover, for the WFC, the components wear-out characteristics is assumed to be $(\alpha, \beta)_{\text{switch}} = (\alpha, \beta)_{\text{cap}} = (12, 3)$, and $(\alpha, \beta)_{\text{switch}} = (\alpha, \beta)_{\text{cap}} = (8, 3)$ respectively for location A and B. According to Fig. 13(a) and (b), the impact of WTC on the time-based unavailability and production-based availability is negligible. Also, the impact of WFC on the time-based unavailability is 74 h/y higher than the base case (168 h/y) in Location B as shown in Fig. 13(a). Therefore, ignoring the impact of WFC and using the historical reliability data will introduce almost 44 % error in time-based unavailability prediction following Fig. 13(a).

Furthermore, as it is shown in Fig. 13(a), the aging parameters of the WFC can affect the unavailability of the WF, where by decreasing α from 12 in location A to 8 in location B, the maximum time-based unavailability is increased from 218 h/y to 242 h/y. The EENP of the WF is illustrated in Fig. 13(c) highlighting the impact of converters wear-out. The aging of WTC will introduce 1,940 MWh/y EENP over the base case which is almost 10%. Furthermore, wear-out of WTCs and WFCs causes 5,080 MWh/y in location A and 7,660 MWh/y in

location B more EENP compared to the base case, which are equal to 27% and 41% of the base case, respectively.

The results in Fig. 13 show that the different WF availability measures are not identical, and may not appropriately show the WF performance. For instance, the impact of WTC wear-out on the time-based unavailability is almost negligible while it can introduce 10% more EENP over the base case. Furthermore, the aging parameters of WTCs and WFCs can affect the reliability of the WF, and thus, need to be modeled in system-level analysis. However, the impact of WFC wear-out is much higher than the impact of WTC. This case study shows that the wind speed profile can affect the converters reliability, and hence, the WF availability. Thus, modeling the converters aging in system-level analysis is of high importance.

Since the converter failure rate is dependent on the operational and environmental conditions, a senility analysis is performed to show the impact of random chance failure rates on the overall performance of WF. Following Fig. 14(a), the FOR of WTC does not affect the time-based unavailability and its impact on the production-based availability is almost negligible as shown in Fig. 14(b). Meanwhile, the WFC considerably affect the time-based unavailability and production-based unavailability of the WF reliability as shown in Fig. 14. Furthermore, the EENP of a 40 MW and 4×40 MW WFs are calculated for the base case which is equal to 4.64 and 18.55 GWh/y respectively. The impact of converters FOR is reported in Fig. 15(a) and (b) respectively. The results show that increasing the WFC FOR remarkably increases the WF EENP, while the impact of WTC on the EENP is not considerable.

C. Power System Reliability

The reliability of modified RBTS and PE-RBTS is evaluated by LOLE and EENS indices. The base case reliability indices are summarized in TABLE II. The LOLE of the RBTS is 1.14 h/y. In order to approximately keep the LOLE to be identical to the base case, the peak load of the system is increased accordingly. This incremental peak load, which is called Peak Load Carrying Capability (PLCC), for modified RBTS is reported in TABLE II. Furthermore, the PLCC for the EP-RBTS is considered as the case of RBTS with 160 MW WF, since the wind capacity penetration in both cases is identical.

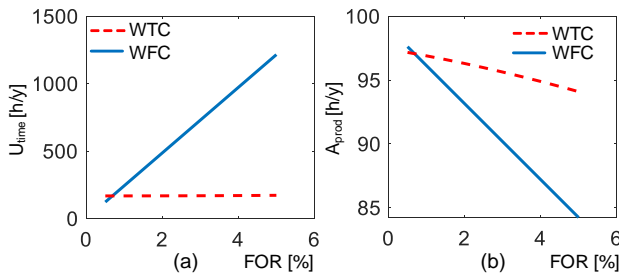


Fig. 14. Impact of WTC and WFC unavailability (FOR) on the (a) time-based unavailability and (b) production-based availability of the WF.

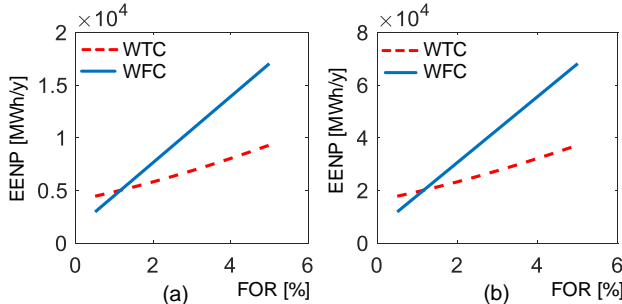


Fig. 15. Impact of WTC and WFC unavailability (FOR) on the EENP by the (a) 40 MW and (b) 160 MW WF.

C.1. Modified RBTS reliability

The impact of WTC and WFC wear-out failure on the system reliability is illustrated in Fig. 16 with the 160 MW WF. First, the aging of WTCs is considered. Following Fig. 16, the WTCs wear-out has negligible impact on the system LOLE and EENS. Next, the aging of both WTCs and WFC is modeled. The obtained results in Fig. 16 shows that the converters aging impact on the LOLE is 2% and EENS is 3%. As a result, for power system-level analysis, the WTCs and WFCs wear-out failure impacts can be neglected.

Moreover, the impact of WTCs and WFCs FOR on the RBTS reliability is shown in Fig. 17(a) and (b) with the 40 and 160 MW WFs. As it can be seen in Fig. 17, increasing the WTC FOR cannot affect the LOLE and EENS with low and high penetration of wind power. However, the system reliability is dependent on the WFC FOR and wind power penetration. As it can be seen in Fig. 17(a), by increasing the WFC FOR with 40 MW WF, the change of LOLE is almost negligible. However, with the 160 MW WF, the impact of WFC FOR on the LOLE is significant as shown in Fig. 17(a). The impact of FOR of converters on the EENS is also similar to the LOLE as shown in Fig. 17(b). Therefore, the WTCs impact on the system reliability is almost negligible, while the WFCs can affect the system reliability especially with high wind power penetration. Thus, the appropriate reliability data of WFCs should be employed in the system-level reliability assessment.

TABLE II

Reliability indices of power system for the base case given in the Appendix.

SYSTEM	RBTS			PE-RBTS
WF Capacity [MW]	0	40	160	160
PLCC [MW]	0	16	65	65
Peak load [MW]	185	201	250	250
Wind penetration [%]	0	20	64	64
LOLE [h/y]	1.14	1.24	1.31	4.10
EENS [MWh/y]	10.00	9.57	12.48	165.00

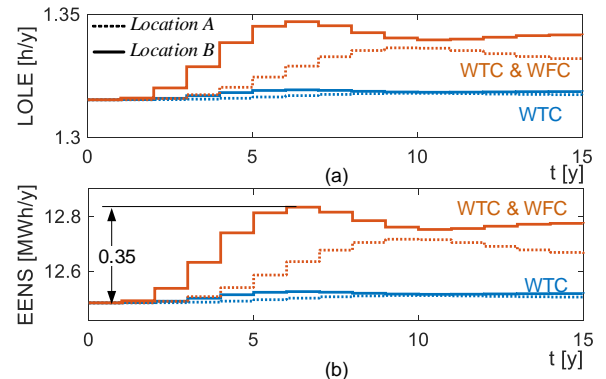


Fig. 16. Impact of WTC and WFC wear-out on the reliability of RBTS with 160 MW WF, (a) LOLE, (b) EENS.

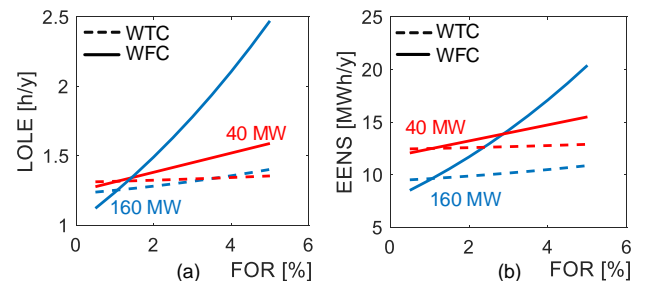


Fig. 17. Impact of WTC and line converter unavailability (FOR) on the (a) LOLE and (b) EENS in RBTS with 40 MW and 160 MW WF.

C.2. Modified PE-RBTS reliability

The reliability of the full power electronic-based system, PE-RBTS shown in Fig. 11 is evaluated in this sub-section. The base case reliability indices have been summarized in TABLE II. Following these results, replacing the conventional generators with HVDC systems connected to the neighboring grids, the base LOLE is increased from 1.31 to 4.10 h/y . Moreover, the system EENS is increased from 12.38 to 165.00 MWh/y . Therefore, moving to full power electronic systems requires HVDC systems with high availability in order to obtain the same performance as the conventional systems.

In order to illustrate the impact of HC aging on the system reliability, the wear-out characteristics of HC converter components are assumed to be $(\alpha, \beta)_{\text{switch}} = (\alpha, \beta)_{\text{cap}} = (8, 3)$. The PE-RBTS LOLE and EENS due to the wear-out failure of WFCs and HCs are shown in Fig. 18. The HCs aging increases the LOLE by 4.5 h/y (109%) and EENS by 190 MWh/y (115%) as shown in Fig. 18(a) and (b). However, the WFCs wear-out impact on LOLE and EENS is negligible.

Moreover, the impact of FOR of HCs and WFCs with 160 MW WF with wind capacity penetration of 654% is shown in Fig. 19. As it can be seen from Fig. 19, the LOLE and EENS are significantly affected by the HC FOR, while the impact of WFCs is negligible. The obtained results show that the random-chance and wear-out failure rate of HC components have significant impact on the overall system reliability.

Therefore, in a full power electronic based power system, accurate reliability analysis requires utilizing appropriate reliability data for random chance failures must be utilized. Moreover, the detailed wear-out failure rate of HC components must be predicted in order to accurately analyze the system reliability. Ignoring the aging of components may introduce erroneous results, consequently non-optimal decision-making within planning and operation of such systems.

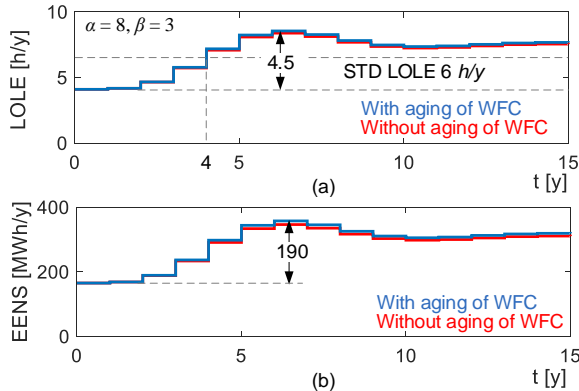


Fig. 18. Impact of WFC and HC wear out on the reliability of FE-RBTS with 160 MW WF, (a) LOLE, (b) EENS.

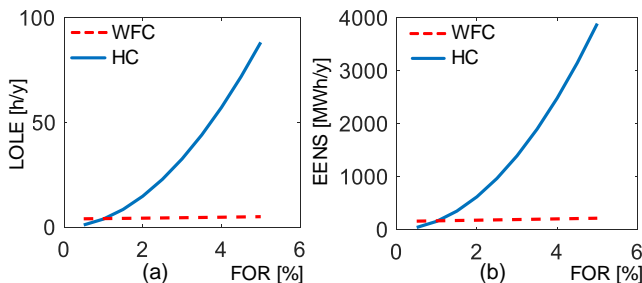


Fig. 19. Impact of WTC and WFC unavailability (FOR) on the (a) LOLE and (b) EENS in PE-RBTS with 40 MW and 160 MW WF.

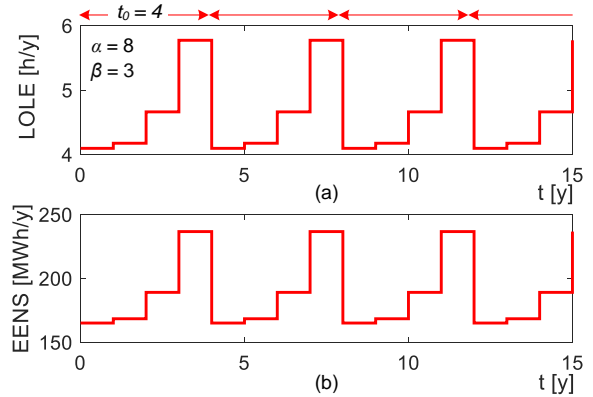


Fig. 20. Impact of the age replacement policy of HC on the reliability of FE-RBTS with 160 MW WF, (a) LOLE, (b) EENS.

C.3. Impact of replacement policy

The LOLE index in a reliable power system must be limited to a standard value, which depends on every country's regulations. For instance, its standard value for European countries is between 4 and 8 h/y [62]. Considering the standard level of 6 h/y , the system performance with the run-to-fail maintenance strategy is not acceptable as shown in Fig. 18(a). Therefore, a proper maintenance strategy such as an age replacement policy must be adopted in order to maintain the system reliability. According to the age replacement policy, the components will be replaced upon failure or specific time t_0 , whichever comes first. Following the system performance shown in Fig. 18(a), the appropriate time of replacement based on the age replacement policy would be the cross points of LOLE curves with the standard level of 6 h/y . As it can be seen from Fig. 18(a), the appropriate planned replacement time t_0 , would be 4 years. As a result, applying the age replacement policy at the planned times, the overall system reliability can be obtained as shown in Fig. 20. It is clear that the time of planned replacement scheduling depends on the wear-out failure characteristics of the HC converters. Therefore, accurate wear-out failure prediction of converters is necessary for appropriate maintenance scheduling in modern power systems.

V. DISCUSSION

The converters are utilized in generation systems such as for wind and solar energy resources, and electronic transmission systems such as HVDC lines. Hence, the converter reliability may affect the overall system reliability according to its applications. Meanwhile, the converters are fragile components and particularly they are prone to aging failures. Thereby, this paper has explored the impact of converter failures on the modern power electronic-based power systems performance. First, the wear-out failure prediction based on SSA in power converters has been presented. Next, the converter reliability model has been incorporated into the power system analysis. Finally, the reliability evaluation in modern power systems has been presented. The impact of converters reliability on the modified RBTS with different proliferation of power converters has been illustrated.

It has been shown that the wear-out failures can affect the converter availability according to the aging parameters. The impact of converter availability on the WF reliability has been illustrated with 20 and 64% wind power penetration. The obtained results have shown that the WTC has negligible impact on the time-based unavailability and production-based availability of WFs. However, its wear-out failure may increase the EENP by 10% compared to the case of neglecting the wear-

out failures. Furthermore, the WFC can highly affect the WF reliability indices. The analysis has shown that the wear-out failure of WFC may introduce almost 45% unavailability over the base case. As a result, the WFC reliability considering the random chance and wear-out failures must accurately be modeled for reliability prediction of WFs. Since, the number of these converters are not too much, e.g., two converters per 40 MW WF, hence, its reliability modeling based on SSA might not be time consuming. However, the number of WTCs is quite high, e.g., 2×40 converters in a 40 MW WF. Thereby, its reliability modeling especially considering different mission profiles for each WT in practice, is almost impossible. As a result, considering the time of analysis with high penetration of WFs, the wear-out reliability of WTCs can be neglected, while it can induce 10% error in the results.

The impact of WTCs and WFCs on the reliability of RBTS with 20% and 64% of wind power penetration has been evaluated. It has been shown that the impact of WTCs and WFCs failures including random chance and wear-out failures on the LOLE and EENS in low and high wind power penetration is almost negligible. Thus, the SSA-based wear-out analysis for the system-level studies for both WTCs and WFCs may not be necessary. However, the WFC FOR can affect the system reliability in high wind power penetration. Therefore, for system reliability analysis, the WFC FOR due to the random chance failures must be appropriately adopted from operation experiences and historical data.

Finally, a modified version of RBTS as a full power electronic system, PE-RBTS is considered with three HVDC links connected to the neighboring countries. The obtained results have shown that the reliability of the system significantly depends on the HVDC system availability. Furthermore, the wear-out failure of HCs has a remarkable impact on the overall system reliability. Therefore, the HC reliability specially the wear-out failures must be accurately modeled for the system-level analysis. Furthermore, the impact of run-to-fail and age replacement policies for HCs has been shown in this paper, where the age replacement policy at a proper time is required to maintain the system reliability under a standard limit.

VI. CONCLUSION

This paper has proposed a procedure to bridge the power electronic and power system reliability concepts. The reliability of power electronic converters is incorporated in power system reliability analysis, which can be beneficial for optimal decision-making within planning, operation and maintenance of modern power systems. The detailed reliability modeling of power electronic-based power systems has been presented from device-level up to power system-level. The impact of converter failure rates on power system performance has been illustrated for different applications. For instance, it has been shown that the wear-out failure of wind turbine converter cannot affect the wind farm and power system performance even under run-to-fail replacement strategy. Moreover, since, the converter reliability modeling in electro-thermal domains is a time-consuming process, the required accuracy in reliability modeling of power converters for different applications has been addressed. This can facilitate the system-level reliability evolution on modern power systems with high proliferation of power converters. Furthermore, the impact of run-to-fail and age replacement policies for power converters on the overall system reliability has been illustrated.

The reliability assessment approach can be easily performed for photovoltaic systems by appropriately modeling the

availability of the solar energy. The remaining analysis will be similar to the wind power plants. Future research will focus on the impact of power management strategies on the system-level reliability of converters. Moreover, appropriate maintenance strategies could be introduced for different applications of converters in power systems.

VII. APPENDIX

The reliability data for base case used in this paper are summarized in TABLE APP-I which are based on the data provided in [3], [38], [39], [63], [64].

TABLE APP-I
Exponential failure and repair rates of WT and HVDC system.

Unit	Sub-system	Component	Failure rate [occ/y]	Repair rate [r/y]
WT	Converter (con.)	Switch	0.15	150
		Capacitor	0.2	150
		Other con. comp.	0.15	185
	Other	Other WT comp.	0.53	200
HVDC	Converter (con.)	Switch	0.3	200
		Capacitor	0.43	50
		Other con. comp.	0.35	10
	Other Comp.	DC Line	0.003	17

REFERENCES

- [1] H. E. Johan, G. W. Steven, and H. Ramtin, "Third EGrid Workshop Maps the Grid of the Future: Attendees Engage to Examine the Role of Power Electronic Applications in Modern Electric Power Systems," *IEEE Power Electron. Mag.*, vol. 6, no. 1, pp. 48–55, 2019.
- [2] S. Yang, A. Bryant, P. Mawby, D. Xiang, L. Ran, and P. Tavner, "An Industry-Based Survey of Reliability in Power Electronic Converters," *IEEE Trans. Ind. Appl.*, vol. 47, no. 3, pp. 1441–1451, May 2011.
- [3] J. Ribrant and L. M. Bertling, "Survey of Failures in Wind Power Systems With Focus on Swedish Wind Power Plants During 1997–2005," *IEEE Trans. Energy Convers.*, vol. 22, no. 1, pp. 167–173, Mar. 2007.
- [4] K. Fischer, K. Pelka, A. Bartschat, B. Tegtmeier, D. Coronado, C. Broer, and J. Wenske, "Reliability of Power Converters in Wind Turbines: Exploratory Analysis of Failure and Operating Data from a Worldwide Turbine Fleet," *IEEE Trans. Power Electron.*, vol. 34, no. 7, pp. 6332–6344, 2018.
- [5] J. Carroll, A. McDonald, and D. McMillan, "Reliability Comparison of Wind Turbines With DFIG and PMG Drive Trains," *IEEE Trans. Energy Convers.*, vol. 30, no. 2, pp. 663–670, Jun. 2015.
- [6] X. Liu and S. Islam, "Reliability Issues of Offshore Wind Farm Topology," *2008 10th Int. Conf. Probabilistic Methods Appl. To Power Syst.*, pp. 523–527, 2008.
- [7] G. J. W. Van Bussel and M. B. Zaaijer, "DOWEC Concepts Study, Reliability, Availability and Maintenance Aspects," *Eur. Wind Energy Conf.*, no. July, pp. 557–560, 2001.
- [8] L. M. Moore and H. N. Post, "Five Years of Operating Experience at a Large, Utility-Scale Photovoltaic Generating Plant," *Prog. Photovoltaics Res. Appl.*, vol. 16, no. 3, pp. 249–259, 2008.
- [9] G. Zini, C. Mangeant, and J. Merten, "Reliability of Large-Scale Grid-Connected Photovoltaic Systems," *Renew. Energy*, vol. 36, no. 9, pp. 2334–2340, 2011.
- [10] A. Golnas, "PV System Reliability: An Operator's Perspective," *IEEE J. Photovoltaics*, vol. 3, no. 1, pp. 416–421, 2013.
- [11] H. S. Chung, H. Wang, F. Blaabjerg, and M. Pecht, "Reliability of Power Electronic Converter Systems," First Edi. London: IET, 2015.
- [12] F. Spinato, P. J. Tavner, G. J. W. van Bussel, and E. Koutoulakos, "Reliability of Wind Turbine Subassemblies," *IET Renew. Power Gener.*, vol. 3, no. 4, p. 387, 2009.
- [13] S. Peyghami, P. Davari, and F. Blaabjerg, "System-Level Reliability-Oriented Power Sharing Strategy for DC Power Systems," *IEEE Trans. Ind. Appl.*, vol. 55, no. 5, pp. 4865–4875, 2019.
- [14] H. S. Chung, H. Wang, F. Blaabjerg, and M. Pecht, "Reliability of Power Electronic Converter Systems." The Institution of Engineering and Technology (IET), 2016.
- [15] Y. Song and B. Wang, "Survey on Reliability of Power Electronic Systems," *IEEE Trans. Power Electron.*, vol. 28, no. 1, pp. 591–604, Jan.

- [16] F. Blaabjerg, K. Ma, and D. Zhou, "Power Electronics and Reliability in Renewable Energy Systems," in *Proc. IEEE ISIE*, 2012, pp. 19–30.
- [17] H. Wang, K. Ma, and F. Blaabjerg, "Design for Reliability of Power Electronic Systems," in *Proc. IEEE IECON*, 2012, pp. 33–44.
- [18] P. D. Reigosa, H. Wang, Y. Yang, F. Blaabjerg, P. D. Reigosa, H. Wang, Y. Yang, and F. Blaabjerg, "Prediction of Bond Wire Fatigue of IGBTs in a PV Inverter under a Long-Term Operation," *IEEE Trans. Power Electron.*, vol. 31, no. 10, pp. 3052–3059, Mar. 2016.
- [19] J. Falck, C. Felgемacher, A. Rojko, M. Liserre, and P. Zacharias, "Reliability of Power Electronic Systems: An Industry Perspective," *IEEE Ind. Electron. Mag.*, vol. 12, no. 2, pp. 24–35, Jun. 2018.
- [20] K. Ma and F. Blaabjerg, "Modulation Methods for Neutral-Point-Clamped Wind Power Converter Achieving Loss and Thermal Redistribution Under Low-Voltage Ride-Through," *IEEE Trans. Ind. Electron.*, vol. 61, no. 2, pp. 835–845, Feb. 2014.
- [21] Y. Wu, M. A. Shafi, A. M. Knight, and R. A. McMahon, "Comparison of the Effects of Continuous and Discontinuous PWM Schemes on Power Losses of Voltage-Sourced Inverters for Induction Motor Drives," *IEEE Trans. Power Electron.*, vol. 26, no. 1, pp. 182–191, Jan. 2011.
- [22] S. Peyghami, H. Wang, P. Davari, and F. Blaabjerg, "Mission Profile Based System-Level Reliability Analysis in DC Microgrids," *IEEE Trans. Ind. Appl.*, vol. 55, no. 5, pp. 5055–5067, 2019.
- [23] M. Andresen, G. Buticchi, and M. Liserre, "Study of Reliability-Efficiency Tradeoff of Active Thermal Control for Power Electronic Systems," *Microelectron. Reliab.*, vol. 58, pp. 119–125, Mar. 2016.
- [24] K. Ma, M. Liserre, and F. Blaabjerg, "Reactive Power Influence on the Thermal Cycling of Multi-MW Wind Power Inverter," *IEEE Trans. Ind. Appl.*, vol. 49, no. 2, pp. 922–930, Mar. 2013.
- [25] Z. Qin, M. Liserre, F. Blaabjerg, and H. Wang, "Energy Storage System by Means of Improved Thermal Performance of a 3 MW Grid Side Wind Power Converter," in *Proc. IEEE IECON*, 2013, pp. 736–742.
- [26] Z. Qin, M. Liserre, F. Blaabjerg, and L. Poh Chiang, "Reliability-Oriented Energy Storage Sizing in Wind Power Systems," in *Proc. IEEE IPEC*, 2014, pp. 857–862.
- [27] S. Peyghami, P. Davari, H. Wang, and F. Blaabjerg, "System-Level Reliability Enhancement of DC/DC Stage in a Single-Phase PV Inverter," *Microelectron. Reliab.*, vol. 88–90, pp. 1030–1035, Sep. 2018.
- [28] S. Peyghami, P. Davari, H. Wang, and F. Blaabjerg, "The Impact of Topology and Mission Profile on the Reliability of Boost-Type Converters in PV Applications," in *Proc. IEEE COMPEL*, 2018, pp. 1–8.
- [29] S. Peyghami, P. Davari, H. Wang, and F. Blaabjerg, "System-Level Reliability Enhancement of DC/DC Stage in a Single-Phase PV Inverter," *Microelectron. Reliab.*, vol. 88–90, pp. 1030–1035, Sep. 2018.
- [30] V. Raveendran, M. Andresen, and M. Liserre, "Improving Onboard Converter Reliability For More Electric Aircraft With Lifetime-Based Control," *IEEE Trans. Ind. Electron.*, pp. 1–10, 2019.
- [31] R. Billinton and R. N. Allan, "Reliability Evaluation of Power Systems," First. New York: Plenum Press, 1984.
- [32] S. Sulaeman, M. Benidris, J. Mitra, and C. Singh, "A Wind Farm Reliability Model Considering Both Wind Variability and Turbine Forced Outages," *IEEE Trans. Sustain. Energy*, vol. 8, no. 2, pp. 629–637, Apr. 2017.
- [33] Y. Guo, H. Gao, and Q. Wu, "A Combined Reliability Model of VSC-HVDC," *IEEE Trans. Sustain. ENERGY*, vol. 8, no. 4, pp. 1637–1646, Oct. 2017.
- [34] C. Maciver, K. R. W. Bell, and D. P. Nedic, "A Reliability Evaluation of Offshore HVDC Grid Configuration Options," *IEEE Trans. Power Deliv.*, vol. 31, no. 2, pp. 810–819, 2016.
- [35] H. J. Bahirat, G. H. Kjolle, B. A. Mork, and H. K. Hoidalén, "Reliability Assessment of DC Wind Farms," *IEEE Power Energy Soc. Gen. Meet.*, pp. 1–7, 2012.
- [36] P. Wang, Z. Gao, and L. Bertling, "Operational Adequacy Studies of Power Systems with Wind Farms and Energy Storages," *IEEE Trans. Power Syst.*, vol. 27, no. 4, pp. 2377–2384, 2012.
- [37] A. S. Dobakhshari and M. Fotuhi-Firuzabad, "A Reliability Model of Large Wind Farms for Power System Adequacy Studies," *IEEE Trans. Energy Convers.*, vol. 24, no. 3, pp. 792–801, 2009.
- [38] Y. Guo, H. Gao, and Q. Wu, "A Combined Reliability Model of VSC-HVDC Connected Offshore Wind Farms Considering Wind Speed Correlation," *IEEE Trans. Sustain. Energy*, vol. 8, no. 4, pp. 1637–1646, Oct. 2017.
- [39] S. Zakhast, M. Fotuhi-Firuzabad, F. Aminifar, R. Billinton, S. O. Faried, and A. A. Edris, "Reliability Evaluation of an HVDC Transmission System Tapped by a VSC Station," *IEEE Trans. Power Deliv.*, vol. 25, no. 3, pp. 1962–1970, 2010.
- [40] JACOBSON, K. L. B., L. J., and M. H. J. BOLLEN, "Reliability Study Methodology for HVDC Grids," *Cigre*, pp. 1–10, 2010.
- [41] H. Yang, Z. Cai, X. Li, and C. Yu, "Assessment of Commutation Failure in HVDC Systems Considering Spatial-Temporal Discreteness of AC System Faults," *J. Mod. Power Syst. Clean Energy*, vol. 6, no. 5, pp. 1055–1065, 2018.
- [42] L. Shen, Q. Tang, T. Li, Y. Wang, and F. Song, "A Review on VSC-HVDC Reliability Modeling and Evaluation Techniques," *IOP Conf. Ser. Mater. Sci. Eng.*, vol. 199, no. 1, 2017.
- [43] A. Albertsen, "Electrolytic Capacitor Lifetime Estimation," *JIANGHAI Eur. GmbH*, pp. 1–13, 2010.
- [44] R. Bayerer, T. Herrmann, T. Licht, J. Lutz, and M. Feller, "Model for Power Cycling Lifetime of IGBT Modules - Various Factors Influencing Lifetime," in *Proc. IEEE CIPS*, 2008, pp. 1–6.
- [45] Cigre Working Group C1.27, "The Future of Reliability - Definition of Reliability in Light of New Developments in Various Devices and Services Which Offer Customers and System Operators New Levels of Flexibility," 2018.
- [46] R. Billinton and R. Allan, "Reliability Evaluation of Engineering Systems." New York: Plenum press, 1992.
- [47] W. R. Nunn and A. M. Desiderio, "Semi-Markov Processes: An Introduction," *Cent. Nav. Anal.*, pp. 1–30, 1977.
- [48] A. Lisnianski, I. Frenkel, and Y. Ding, "Multi-State System Reliability Analysis and Optimization for Engineers and Industrial Managers." London: Springer London, 2010.
- [49] J. Falck, C. Felgемacher, A. Rojko, M. Liserre, and P. Zacharias, "Reliability of Power Electronic Systems," *IEEE Ind. Electron. Mag.*, vol. 12, no. 2, pp. 24–35, 2018.
- [50] F. A. Bhuiyan and A. Yazdani, "Reliability Assessment of a Wind-Power System with Integrated Energy Storage," *IET Renew. Power Gener.*, vol. 4, no. 3, p. 211, 2010.
- [51] IEC61400-26-1, "Part 26-1: Time-Based Availability for Wind Turbine Generating Systems," 2011.
- [52] IEC61400-26-2, "Part 26-2: Production-Based Availability for Wind Turbines," 2014.
- [53] IEC61400-26-3, "Part 26-3: Availability for Wind Power Stations," 2016.
- [54] Y. V. Makarov, "Probabilistic Assessment of the Energy Not Produced Due to Transmission Constraints," in *Proc. IEEE Power Tech Conference*, 2003, pp. 435–437.
- [55] R. Billinton and K. Chu, "Early Evolution of LOLP: Evaluating Generating Capacity Requirements [History]," *IEEE Power Energy Mag.*, vol. 13, no. 4, pp. 88–98, Jul. 2015.
- [56] R. Billinton and P. G. Harrington, "Reliability Evaluation in Energy Limited Generating Capacity Studies," *IEEE Trans. Power Appar. Syst.*, vol. PAS-97, no. 6, pp. 2076–2085, 1978.
- [57] R. Billinton, S. Kumar, N. Chowdhury, K. Chu, K. Debnath, L. Goel, E. Khan, P. Kos, G. Nourbakhsh, and J. Oteng-Adjei, "A Reliability Test System for Educational Purposes-Basic Data," *IEEE Power Eng. Rev.*, vol. 9, no. 8, pp. 67–68, 1989.
- [58] D. Zhou, F. Blaabjerg, M. Lau, and M. Tonnes, "Thermal Cycling Overview of Multi-Megawatt Two-Level Wind Power Converter at Full Grid Code Operation," *IEEJ J. Ind. Appl.*, vol. 2, no. 4, pp. 173–182, 2013.
- [59] S. Peyghami, Z. Wang, and F. Blaabjerg, "Reliability Modeling of Power Electronic Converters: A General Approach," in *Proc. IEEE COMPEL*, 2019, pp. 1–7.
- [60] K. Ma, M. Liserre, F. Blaabjerg, and T. Kerekes, "Thermal Loading and Lifetime Estimation for Power Device Considering Mission Profiles in Wind Power Converter," *IEEE Trans. Power Electron.*, vol. 30, no. 2, pp. 590–602, Feb. 2015.
- [61] P. D. Reigosa, H. Wang, Y. Yang, and F. Blaabjerg, "Prediction of Bond Wire Fatigue of IGBTs in a PV Inverter under a Long-Term Operation," *IEEE Trans. Power Electron.*, vol. 31, no. 10, pp. 3052–3059, Mar. 2016.
- [62] M. Čepin and M. Cepin, "Assessment of Power System Reliability Methods and Applications." Springer London Dordrecht Heidelberg New York, 2011.
- [63] B. Hahn, M. Durstewitz, and K. Rohrig, "Reliability of Wind Turbines - Experience of 15 Years with 1500WTs," *Wind Energy*, no. January, pp. 329–332, 2005.
- [64] C. J. Crabtree, D. Zappalá, and S. I. Hogg, "Wind Energy: UK Experiences and Offshore Operational Challenges," *J. Power Energy*, vol. 229, no. 7, pp. 727–746, 2015.